

A New Method for Cartridge Case Image Mosaic

Man Luo^{1,2}, Miao Qi^{1,*}

¹School of Computer Science and Information Technology, Northeast Normal University, Changchun, China

²College of Air Traffic Management, Civil Aviation University of China, Tianjin, China

luoman319@126.com

Abstract—In the process of cartridge case marks detection, due to the limitations of microscope and the unsmoothed specimen surface, not all information can be obtained from just one image. Therefore, two kinds of images can be first obtained and then the information can be supplemented by image mosaic method which facilitates experts' analysis and the following computer recognition. This paper proposes a new cartridge case image mosaic method by using image registration and fusion techniques. In the registration stage, the initial matching is obtained by using scale invariant feature transform (SIFT), but some incorrect matches greatly affect the registration accuracy. Therefore, in consideration of the specific characteristics of the cartridge case image, graph transformation matching, angle and scale constraint using adaptive K-means clustering are respectively applied to remove incorrect matches. In order to achieve the complementary advantages, voting mechanism is applied to integrate them; meanwhile, genetic algorithm (GA) is employed to select optimal combined parameters, making it possible to adaptively choose to integrate and registration results are optimized based on different images. After refining, the registration accuracy is further enhanced. In the fusion stage, the stitched image is obtained, and histogram matching is employed to smooth visible seams. The mosaic performance is evaluated using visual inspection and objective performance measurements, and results show the advantages of proposed method compared to conventional method.

Keywords—image mosaic; image registration; image fusion; removing of incorrect feature matching; voting mechanism; genetic algorithm

I. INTRODUCTION

When a firearm is loaded and fired, characteristic marks appear as bullet striation and impression left on cartridge case, which can be viewed as “fingerprints” for identification of a firearm [1]. In recent years, the analysis of cartridge case marks based on image processing and pattern recognition is developing very fast and plays an important role in the forensic ballistics[2]. However, due to the limitations of microscope (such as vision, depth of field and focal length, etc.) and the unsmooth specimen surface, it is difficult to acquire high resolution images of both local details and global structure of the cartridge case at the same time [3]. These requirements can be achieved by acquiring two kinds of images (see Fig. 1). On the right column, the scope of the

images is large enough to accommodate the whole structure to be analyzed. But the resolution of the local details (such as firing pin impression) is often insufficient, while images on the left have problems with overall structure. In this case, we apply the image mosaic [4] to integrate them into a single composite image, through which a more informative image can be obtained. Undoubtedly, it facilitates firearm experts' analysis through visual inspections and the following computer processing.

Generally, the process of image mosaic falls into two steps: image registration and image fusion, and image registration is very crucial [5]. Registration methods can be divided into two categories: feature-based and the area-based techniques. For their simplicity and reliability, the feature-based methods are employed in most cases. In recent years, the scale and affine invariant features are presented, and a comparison of many modern feature-based techniques [6] found that scale-invariant feature transform (SIFT) [7] outperformed other available techniques in most tests. However, because of the similar texture of cartridge case, the initial SIFT matching always contains some incorrect matches, for which an incorrect transformation matrix will occur and can lead to wrong results accordingly. Due to the unknown distribution of incorrect matches, the work of removing incorrect matches is the main difficulty and research focus of this paper. After registration, the seamless stitched image is obtained by pixel-level fusion.

The rest of the paper is organized as follows. In Section 2 an efficient mosaic method is presented. Then Section 3 explains the experiment results and discussion. Finally, the conclusions are summarized in Section 4.

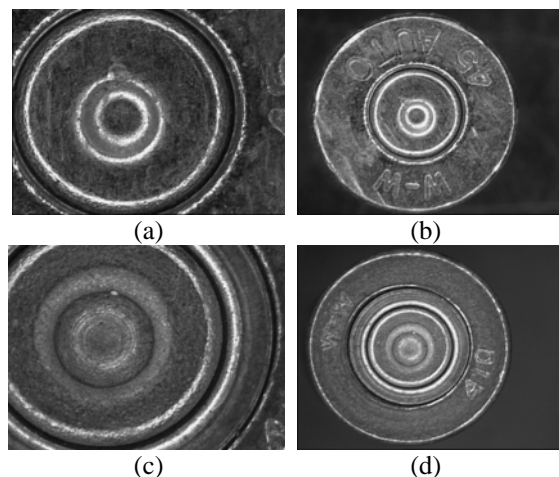


Figure 1. Some examples of cartridge case image.

* Corresponding author
Email:qim801@nenu.edu.cn
Tel.: +86 431 84536326
Fax: +86 431 85696533

II. CARTRIDGE CASE IMAGE MOSAIC METHOD

A. Cartridge Case Image Set

The image data in this paper come from real cartridge cases, and the cartridge cases bear much repetition and similarity. 26 pairs of images are within the Image Set and marked with digits like Pair-1, Pair-2 etc. Here, some examples are shown in Fig. 1. The reference images with clear local details (e.g. firing pin impression) are on the left column, and the sensed images which demonstrate the global structure are on the right column. The reference image and the sensed image are of the same size (480×640). From Fig. 1, it is found that the 2 images of each cartridge case specimen have all undergone scaling, and even some of them undergone rotating.

B. SIFT Feature Extraction and Matching

SIFT features are invariant to scaling, rotations and changes in illumination, and they consist of two major stages [8]. In the first stage, SIFT uses a sequential filtering technique that gradually selects keypoints. In the second stage, for each keypoint, it generates a set of descriptors using local image gradients within the neighborhood at a selected scale. This feature extraction is performed on both the reference and the sensed image.

For the built descriptor in reference image, the matching process may be performed by finding the first and second closest neighbor of each keypoint in sensed image's keypoint descriptor set. If the value between keypoint and its first closest neighbor is less than $th1=0.15$, and also the ratio between first and second closest neighbor is less than $th2=0.75$, the keypoint with first closest neighbor is considered as the best match point.

C. Removing Incorrect Matches

From the above process, two sets of corresponding points, that is, $Q=\{q_i\}$ in the reference image, and $Q'=\{q'_i\}$ in the sensed image, $i=1,2,\dots,N$ (where q_i matches q'_i) are found. Because of the similar textures on cartridge cases, several of the corresponding pairs are likely to be incorrect, which might lead to unexpected and unacceptable registration results. Therefore, the outliers-removing algorithm is so important that it determines the accuracy of the results.

1) *Graph Transformation Matching (GTM)*: Graph Transformation Matching (GTM) [9] is an effective and fast algorithm to remove incorrect matches that uses the local structure information and its principle is to enforce coherent spatial relationship of corresponding points between both images. Compared to other methods, such as RANSAC+epipolar geometry and softassign, GTM has been proven to be remarkable by experimental evaluation. When the matches are all correct, the median K-nearest-neighbor (KNN) graphs $G(Q)$ and $G(Q')$ are isomorphic, otherwise, the structure of $G(Q)$ is different from that of $G(Q')$. So the GTM algorithm is designed to iteratively remove incorrect matches which destroy

coherent spatial relationships. Finally, surviving elements of two sets are correct matches. Here, Fig.2 is an example, from iteration 0 (initial graphs) to iteration 5 (final identical graphs), with $K=4$. However, Reference [9] points out the few incorrect matches that are not discarded are actually close to correct matches by using GTM.

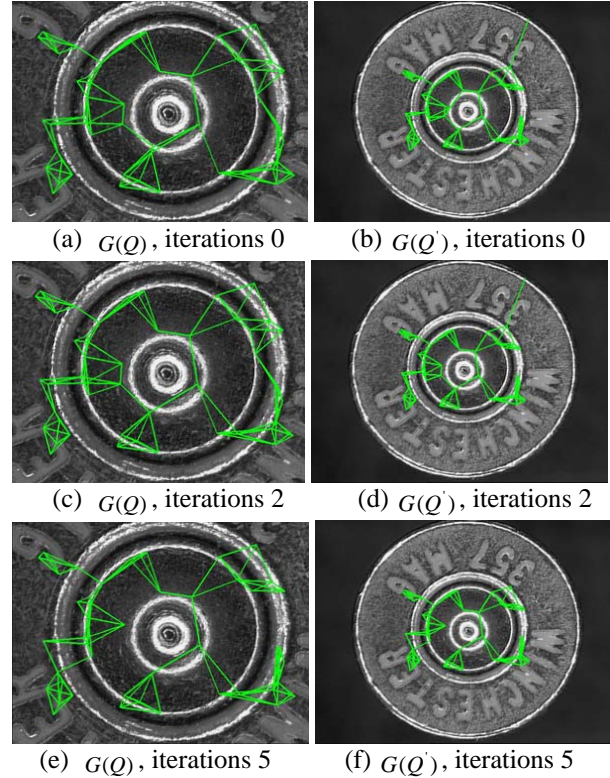


Figure 2. Graph transformation process example.

2) *Angle constraint and scale constraint using adaptive K-means clustering*: Because scaling alone or both scaling and rotation occur between the reference image and sensed image, a robust technique based on geometric constraint is applied to remove incorrect matches.

Firstly, select a salient point p in the reference image, and p' is the corresponding correct match to p in the sensed image, and they are homonymy points. Secondly, connect p with q_i and obtain a vector v_i , where an angle θ_i is between v_i and horizontal direction, d_i is the Euclidean distance between p and q_i . Similarly, θ'_i and d'_i correspond to θ_i and d_i in the sensed image. The difference between θ_i and θ'_i is called rotation angle feature $\hat{\theta}_i$, and the corresponding feature set $\hat{\theta}$ is defined as follows:

$$\hat{\theta} : \{\hat{\theta}_i = \theta_i - \theta'_i, i = 1, \dots, N\}. \quad (1)$$

Similarly, the scale zoom ratio feature R_i and the corresponding feature set R are defined as follows:

$$R : \{R_i = d_i/d'_i, i = 1, \dots, N\}. \quad (2)$$

The rotation angle features of the correct matches should be very similar to one another and so should the scale zoom ratio feature be. They are called angle constraint and scale constraint for short in this paper.

Now, removing incorrect matches can be considered as the process of clustering, and K-means clustering [10] is suitable for solving this task. Due to the individuation of each image, the distribution of the incorrect matches is not a priori, so it cannot be given certain cluster number. An adaptive method of identifying the initial cluster center is provided [11]. The angle constraint algorithm using adaptive K-means clustering is as follows:

Step1: Define initial cluster boundary: Select the threshold $th3$ as the initial cluster boundary and sort elements of set $\hat{\theta}$ in ascending order.

Step2: Identify initial cluster center: Scan the elements of set $\hat{\theta}$ in sequence, and if the $\hat{\theta}_i - \hat{\theta}_{i-1} < th3$, they are marked for the same cluster, otherwise $\hat{\theta}_i$ is marked for a new cluster. Repeat this process until the end of the scan. The respective mean value of each cluster is defined as the corresponding initial cluster center, which is used in the K-means clustering.

Step3: Obtain correct matching: Select the cluster with the largest number of elements after K-means clustering, and the keypoints matching which this cluster corresponds to is correct matching.

The scale constraint algorithm using adaptive K-means clustering is similar to the angle constraint algorithm, and the threshold is $th4$.

3) *Voting mechanism*: The voting mechanism is a kind of decision fusion mode, and it contains various forms, such as ‘and’ or ‘or’ rule and so on. ‘And’ rule is applied in this paper. In order to achieve the complementary advantages, the voting mechanism combines GTM, angle constraint and scale constraint. For each initial matching, when GTM, angle constraint and scale constraint in the voting mechanism all agree it is the correct matching, it is viewed as the correct matching. In addition, for the sake of comparison to the combination of three methods, we take the voting mechanism and only combine angle constraint and scale constraint, and call this method dual-feature constraint in this paper.

4) *Genetic algorithm*: As to the cartridge case images in this paper, the parameters range in angle constraint, scale constraint and GTM are respectively $th3 = 1^\circ, 2^\circ, 3^\circ, 4^\circ, 5^\circ$, $th4 = 0.01, 0.02, 0.03, 0.04, 0.05$ and $K = 2, 3, 4, 5, 6$. Different ways of combination of the parameter values lead to different results when the voting mechanism combining GTM, angle constraint and scale constraint is applied. Therefore, Genetic algorithm (GA) [12] can be employed to solve such problems to obtain optimal or sub-optimal solution. The choice of fitness function is a crucial step in GA, and it is defined as the process of registration accuracy value being made highest by combination of these parameter values in the voting mechanism. Moreover, special parameter values are defined in the voting mechanism as follows: when $th3 = 0^\circ$ or $th4 = 0$, the respective angle constraint or scale constraint result is still the SIFT initial matching. Similarly, $K = 0$, the respective results are also the initial matching. The purpose of doing so is to implicitly include the choice of methods which are involved in the

voting mechanism. That is, during the process of the voting mechanism based on the three methods, the comparison of NMI occurs among the single method, arbitrary combination of two methods and combination of three methods, when the parameters of theirs respectively change. The above mentioned process makes it possible to adaptively choose to integrate and incorrect matches are removed effectively based on different images.

D. Spatial Transformation

As soon as correct matches through the voting mechanism are identified, the affine transform matrix is illustrated in (3) and is estimated by using a robust least squares approach.

$$\begin{pmatrix} x' \\ y' \\ 1 \end{pmatrix} = \begin{pmatrix} h_{11} & h_{12} & h_{13} \\ h_{21} & h_{22} & h_{23} \\ 0 & 0 & 1 \end{pmatrix} \begin{pmatrix} x \\ y \\ 1 \end{pmatrix} \tag{3}$$

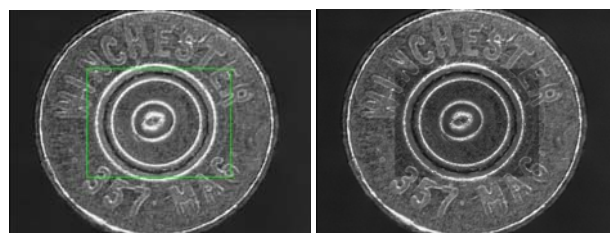
Then each pixel of the sensed image will undergo geometric transformation to the new coordinates of reference image, that is, the sensed image after registering(the registered image) is obtained (see Fig. 3(a)).

E. The Refining of Registraion Result

After the above steps, the registration result is obtained. e.g., between the reference image and the registered image, the top left corner of overlapping region where the coordinate position (x, y) of the pixel g is chosen. In order to validate the current result or obtain a more refined result, the registered image is made floating slightly on the reference image within 3×3 neighborhood of pixel g . If g' is within the neighborhood of g , when floating, g' taking place of g as top left corner of overlapping region and making registration accuracy highest, the corresponding result is refined result.

F. Image Fusion to Obtain Stitched Image

After the registration, the reference image corresponds to the local region (e.g., the green box in the Fig. 3(a)) in the registered image, and this local region is called overlapping region. Because the reference image bears high-resolution local details (such as firing pin impression), the pixels of overlapping region in the stitched image are from reference image, and the pixels of remaining region are from the registered image. After the above process, the reference image and the registered image are merged together to form a single stitched image (e.g., Fig. 3(b)).



(a)the registered image (1010×1344);(b) the stitched image(1010×1344)

Figure 3. The illustration of the stitched image

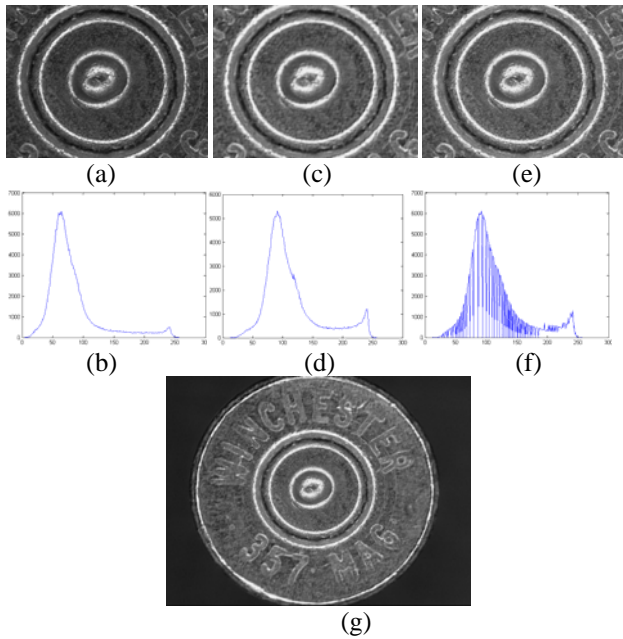


Figure4. The illustration of the histogram matching.

G. Smoothing Seams In Stitched Image

During the image acquisition, the illumination intensity may change, so the overlapping region and other region show undesirable intensity discrepancies in the stitched image in most cases. In order to eliminate such effects and improve visual quality of the stitched image, the histogram matching technology [13] is applied to smooth visible seams. For example, the histogram h of the reference image (Fig. 4 (a)) is illustrated in Fig. 4 (b), and Fig. 4 (c) is the overlapping region of registered image, the histogram h' of Fig. 4 (c) which is the goal of histogram matching is illustrated in Fig. 4 (d), that is to, by histogram matching method, transform h to h'' (Fig. 4 (f)). Fig. 4 (e) is the reference image after histogram transforming, and the appearance of the h'' is similar to h' , the intensity of Fig. 4 (e) is close to Fig. 4 (c). Therefore, the histogram matching method is performed to make seams in the stitched images visually undetectable.

III. EXPERIMENT RESULTS

A. Image Registration Results

The true transform matrix between the reference image and the sensed image are unknown. Therefore, the normalized mutual information (NMI) [14] criterions are employed to evaluate registration accuracy, which is calculated as follows:

$$NMI(F, R) = \frac{H(F) + H(R)}{H(F, R)} \tag{4}$$

where

$$H(F) = -\sum_{i \in F} P_F(i) \log P_F(i)$$

$$H(R) = -\sum_{j \in R} P_R(j) \log P_R(j)$$

$$H(F, R) = -\sum_{i \in F, j \in R} P_{RF}(i, j) \log P_{RF}(i, j)$$

F is overlapping region of the registered image (e.g., Fig. 4(c)), R is the reference image (e.g., Fig. 4(a)). $H(F)$, $H(R)$ is the marginal entropy for each image, and $H(F, R)$ is the joint entropy of the two images. Normalized mutual information conception comes from information theory, and it is the robust evaluation standards of registration accuracy. In general, the higher the value of NMI, the higher the accuracy of the image registration result.

In order to analyze the performance of the proposed mosaic method, an Image Set with 26 pairs of images is applied to do experiment.

After SIFT matching, the initial matching between the each image pair is obtained. 16 over 26 pairs of images have no incorrect matches (e.g., Fig. 5(a)), they are called Image Set I and the corresponding registration results (e.g., Fig. 5(b)) are acceptable, therefore the refining process may be performed directly. However, some incorrect matches (e.g., Fig. 5 (c)) remain in the other 10 pairs of images, which produce incorrect transformation matrix. They can lead to wrong results (e.g., Fig. 5 (d)). In addition, the results that are evaluated objectively by using NMI are shown in Table I. If the $NMI \leq 1.10$, the result is wrong or inaccurate. This threshold value is chosen by visually assessing the registration results. And the 10 pairs of images with incorrect matches are called Image Set II, and marked in boldface in Table I.

TABLE I. THE RESULTS OF INITIAL SIFT MATCHING

Image Pair	Number of initial matching	NMI	Image Pair	Number of initial matching	NMI
Pair-1	50	1.0358	Pair-14	19	1.1103
Pair-2	36	1.0211	Pair-15	30	1.1085
Pair-3	34	1.1279	Pair-16	110	1.0464
Pair-4	53	1.1237	Pair-17	41	1.1053
Pair-5	18	1.0448	Pair-18	67	1.1113
Pair-6	13	1.1308	Pair-19	57	1.0381
Pair-7	30	1.0542	Pair-20	51	1.1028
Pair-8	45	1.1370	Pair-21	19	1.0543
Pair-9	62	1.1355	Pair-22	34	1.1186
Pair-10	22	1.0162	Pair-23	70	1.0712
Pair-11	30	1.1172	Pair-24	49	1.1281
Pair-12	26	1.1108	Pair-25	74	1.1335
Pair-13	14	1.1010	Pair-26	46	1.0462

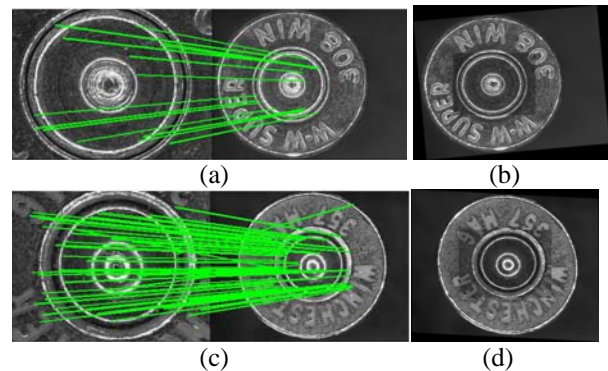


Figure5. The initial SIFT matching and corresponding results.

Then GTM, angle constraint and scale constraint are respectively applied to remove incorrect matches on the

Image Set II, and corresponding registration results by using NMI evaluation are listed in Table II, Table III and Table IV. The optimal result achieved by adjusting parameters is marked bold when three methods are applied. By comparing the results in Table II, Table III and Table IV, GTM and angle constraint algorithms are found to be robust to most image pairs when the parameters *K* and *th3* change, and most of the registration results are good. On the contrary, the results by scale constraint is sensitive to parameter change, but there are examples where the registration results of image pairs are better than those of GTM and Angle constraint, such as Pair-21. Therefore, it is recommended to use GTM method and Angle constraint when each of the three methods is used alone.

TABLE II.
THE RESULTS OF SIFT+ ANGLE CONSTRAINT

Image Pair	NMI				
	<i>th3</i> = 1°	<i>th3</i> = 2°	<i>th3</i> = 3°	<i>th3</i> = 4°	<i>th3</i> = 5°
Pair-1	1.1045	1.1214	1.1214	1.1214	1.1214
Pair-2	1.1217	1.1185	1.1185	1.1185	1.1185
Pair-5	1.1216	1.1382	1.1045	1.1045	1.1045
Pair-7	1.142	1.1510	1.1510	1.1510	1.1510
Pair-10	1.1141	1.1157	1.1216	1.1216	1.1216
Pair-16	1.1342	1.1464	1.1464	1.1464	1.1464
Pair-19	1.1323	1.1323	1.1323	1.1323	1.1323
Pair-21	1.1185	1.1242	1.1242	1.1242	1.1242
Pair-23	1.1305	1.1447	1.1447	1.1447	1.1447
Pair-26	1.1031	1.1288	1.1288	1.1288	1.1288

TABLE III.
THE RESULTS OF SIFT+ SCALE CONSTRAINT

Image Pair	NMI				
	<i>th4</i> = 0.01	<i>th4</i> = 0.02	<i>th4</i> = 0.03	<i>th4</i> = 0.04	<i>th4</i> = 0.05
Pair-1	1.1143	1.1143	1.0151	1.0358	1.0358
Pair-2	1.1211	1.0114	1.0211	1.0211	1.0211
Pair-5	1.0323	1.0414	1.0414	1.0414	1.0414
Pair-7	1.1159	1.0517	1.0517	1.0517	1.0517
Pair-10	1.1224	1.1155	1.1155	1.1155	1.1155
Pair-16	1.0391	1.1328	1.1328	1.0463	1.0463
Pair-19	1.1292	1.1323	1.1323	1.1323	1.0896
Pair-21	1.1343	1.1343	1.0543	1.0543	1.0543
Pair-23	1.1441	1.1217	1.1341	1.1341	1.1341
Pair-26	1.1148	1.1219	1.1219	1.0462	1.0462

TABLE IV.
THE RESULTS OF SIFT+ GTM

Image Pair	NMI				
	<i>K</i> =2	<i>K</i> =3	<i>K</i> =4	<i>K</i> =5	<i>K</i> =6
Pair-1	1.1131	1.1117	1.1131	1.1033	1.1214
Pair-2	1.1103	1.1186	1.1186	1.1177	1.1186
Pair-5	1.0422	1.0908	1.0805	1.0821	1.0969
Pair-7	1.1510	1.1510	1.1510	1.1510	1.1421
Pair-10	1.1216	1.1214	1.1216	1.1180	1.1240
Pair-16	1.1465	1.1467	1.1466	1.1463	1.1466
Pair-19	1.1323	1.1323	1.1323	1.1323	1.1324
Pair-21	1.1277	1.1277	1.1277	1.1319	1.1320
Pair-23	1.1449	1.1449	1.1299	1.1335	1.1449
Pair-26	1.1196	1.122	1.1304	1.1304	1.1195

Now, the voting mechanism that combines GTM, angle constraint and scale constraint is applied to remove incorrect matches on the Image Set II. Similar to the methods mentioned before, the dual-feature constraint is used for comparison. The main parameters of GA are as

follows: population size is 20, crossover rate is 0.25, mutation rate is 0.03, and training iterations are 20.

The registration results of the dual-feature constraint are listed in Table V, such as Pair-16, Pair-19, and Pair-23, their results are better than the best between angle constraint and scale constraint independent operation. Moreover, the results of other images equal those best of angle constraint and scale constraint, and are equivalent to the optimum chosen between the two methods, which is better than a single method.

The registration results of the voting mechanism are listed in Table VI. And the results marked in boldface are better than the best among those of three methods when respective parameters change, and there are totally 7 pairs, such as Pair-2, Pair-5...Pair-23 and so on. In addition, the results of the remainder in Table VI are also equal to the best among three methods.

TABLE V.
THE RESULTS OF SIFT+ DUAL- FEATURE CONSTRAINT

Image Pair	Th3 (degree)	Th4	NMI		
			SIFT result	SIFT+ dual-feature constraint	optimality between angle and scale constraint
Pair-1	2	0.04	1.0358	1.1214	1.1214
Pair-2	1	0.03	1.0211	1.1217	1.1217
Pair-5	2	0	1.0448	1.1382	1.1382
Pair-7	2	0	1.0542	1.1510	1.1510
Pair-10	3	0.01	1.0162	1.1224	1.1224
Pair-16	1	0.01	1.0464	1.1553	1.1464
Pair-19	1	0.01	1.0381	1.1358	1.1323
Pair-21	4	0.02	1.0543	1.1343	1.1343
Pair-23	1	0.01	1.0712	1.1585	1.1447
Pair-26	2	0	1.0462	1.1288	1.1288
Mean value			1.0428	1.1367	1.1341

TABLE VI.
THE RESULTS OF SIFT+ VOTING MECHANISM

Image Pair	Th3	Th4	<i>K</i>	NMI		
				SIFT result	SIFT+ voting mechanism	optimality among three methods
Pair-1	2	0.05	0	1.0358	1.1214	1.1214
Pair-2	2	0.01	5	1.0211	1.1228	1.1217
Pair-5	2	0.02	6	1.0448	1.1521	1.1382
Pair-7	0	0	2	1.0542	1.1510	1.1510
Pair-10	1	0.03	6	1.0162	1.1297	1.1240
Pair-16	2	0.01	6	1.0464	1.1673	1.1467
Pair-19	1	0.01	5	1.0381	1.1430	1.1324
Pair-21	2	0.01	4	1.0543	1.1343	1.1343
Pair-23	1	0.01	0	1.0712	1.1585	1.1449
Pair-26	3	0.01	3	1.0462	1.1319	1.1304
Mean value				1.0428	1.1412	1.1345

Fig. 6 shows the comparison among SIFT, SIFT+ dual-feature constraint and SIFT+voting mechanism, all the 10 pairs of images obtain accurate results after dual-feature constraint or voting mechanism. From Fig. 6, most of the voting mechanism results are better than those of based on the dual-feature constraint, and the remainder results are equivalent.

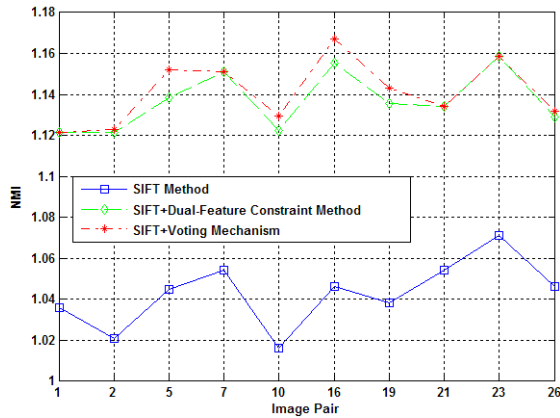


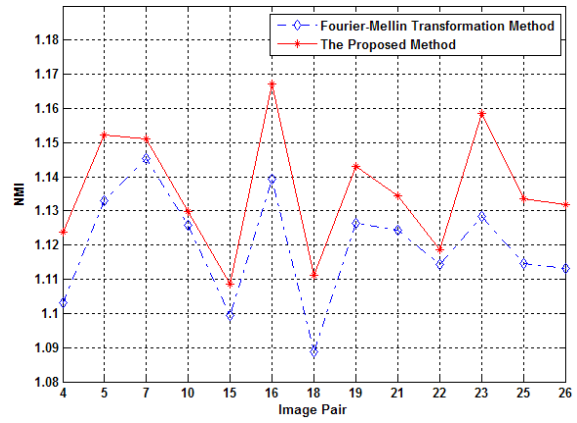
Figure 6. The comparison among SIFT, SIFT+ dual-feature constraint and SIFT+ Voting Mechanism.

To sum up, the voting mechanism achieves the complementary advantages between three methods based on different images, and it proved effective in removing incorrect matching and registration accuracy is enhanced.

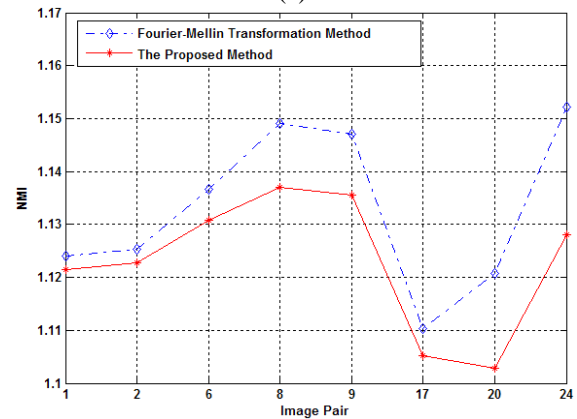
Furthermore, an experiment is performed by employing the Fourier–Mellin transform (FMT) [15] registration method in order to compare with the proposed registration method in Image Set. Image registration based on FMT is different from the traditional area-based method and has characteristic of relatively high robustness in terms of consistent illumination change and noise, and meanwhile high registration accuracy and fast computation[16]. In some special circumstances, however, for example, strong noise caused by severe spectrum aliasing when rotating, plus the similarity of cartridge case image pattern and partial overlapping between images, and despite improvement by high pass filter and window function etc., sometimes the spatial transformation parameters are still unusual and unacceptable by subjective observation, therefore the registration is considered a failure.

The FMT method is also applied to the whole Image Set (26 pairs), and 5 pairs failed, namely Pair 3, Pair 11, Pair 12, Pair 13 and Pair 14 and the NMI value is not calculated to evaluate anymore. Therefore, in terms of the robustness of methods, the proposed method is more suitable for cartridge case image set. Among the 21 effective pairs of images by means of FMT, the registration accuracy of 13 pairs in Fig. 7 by proposed method is better than FMT method, while FMT is more accurate for the rest 8 pairs in (b). The average of NMI value ($NMI=1.1308$) of proposed method is also better than that of FMT method ($NMI=1.1248$). In a word, the proposed method built high accuracy and robust registration results.

In Fig.8, the blue triangles are the registration results of original SIFT method, while red stars are the results by the proposed method+ refining. (refining results in short) We can see that after refining alone (Image Set I) or both voting mechanism and refining (Image Set II) step and compared to the original SIFT method, the registration accuracy of all images in the Image Set is enhanced accordingly.



(a)



(b)

Figure 7. The comparison between FMT and the proposed method.

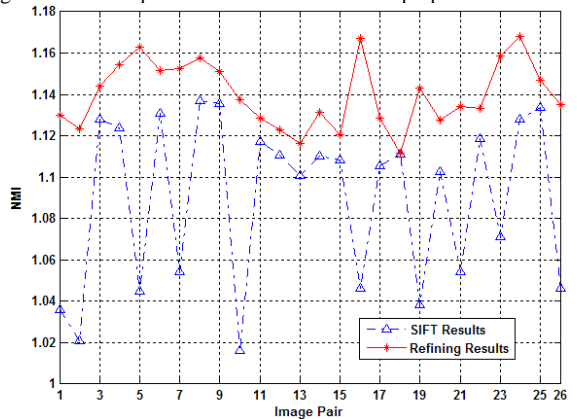


Figure 8. The comparison between SIFT and Refining Result.

B. Image Fusion Results

Firstly, we visually observe Figure 9, where Fig. 9 (a) (size: 480×640) is the reference image with detailed features of firing pin impression. However it has a problem of not containing the global structure of the cartridge case bottom and Fig. 9(b) (size: 480×640) is the sensed image with problems opposite to those of Fig. 9(a). (c) is the stitched image after smoothing(size: 1041×1352), (d) illustrates that sensed image after rotating and scaling which are with the same size of the stitched images(Fig. 9(c)).The partial enlargement (c) and (d) are shown in (e) and (f), (e) is clearer, and contains more details from the visual aspect. To conclude, we can integrate information from both of them into a stitched image which contains both the global structure and local

details of the cartridge case by employing our mosaic algorithm.

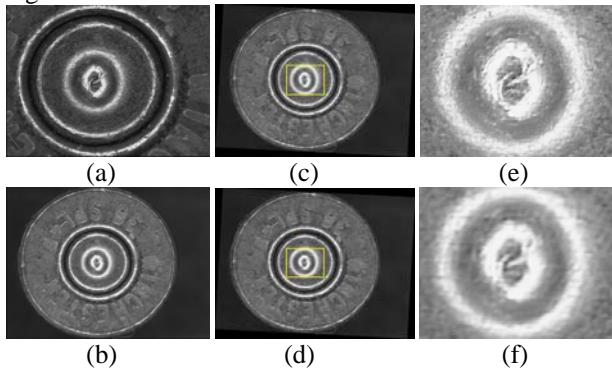


Figure 9. The illustration of the image fusion .

Secondly, the Energy of Laplacian (EOL) [17] and Discrete Cosine Transformation (DCT) are applied to evaluate objectively the fusion results.

1) *Energy of Laplacian (EOL)*: The EOL indicates the sharpness of images and directly reflects the clearness of images and indirectly shows the information contained in the images.:

$$EOL = \sum_x \sum_y (f_{xx} + f_{yy})^2, \quad (5)$$

where

$$\begin{aligned} f_{xx} + f_{yy} = & -f(x-1, y-1) - 4f(x-1, y) - f(x-1, y+1) \\ & - 4f(x, y-1) + 20f(x, y) - 4f(x, y+1) - f(x+1, y-1) \\ & - 4f(x+1, y) - f(x+1, y+1). \end{aligned} \quad (6)$$

If the image is of poor quality, the EOL value is low. After a great many experiments in Reference [17], EOL proved to be better than various methods like Variance, Energy of image gradient, Spatial Frequency and so on.

2) *Discrete cosine transformation (DCT)*: DCT [18] converts the information of a block in spatial domain into frequency domain, and the spectrums are divided into three sub-bands, namely low-frequency, medium frequency and high frequency. The ratio of DCT spectrum concentration on high frequency sub-band is defined as follows:

$$R_H = \frac{E_H}{E_L + E_M + E_H} \quad (7)$$

where $E_j, j=L, M, H$, is the spectral energy concentration on sub-band respectively. The larger the ratio is, the more detail information an image contains. In addition, the block sharpness assessment using R_H performs better than DWT [18].

The EOL and R_H values are computed both of the stitched images after smoothing and sensed image after transforming (rotating and scaling) which are with the same size of the stitched images. And the corresponding comparison results in the Image Set are shown in the Fig. 10. Obviously, all the former are higher than the latter. Therefore, the stitched image combining the supplementary information of reference image and sensed image makes it easier for experts' analysis and computer processing of cartridge cases.

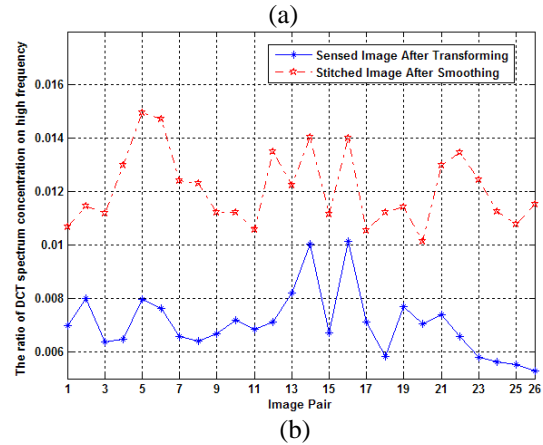
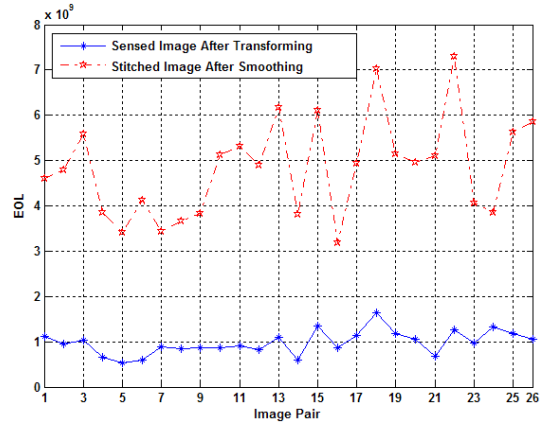


Figure 10. The comparison results of EOL and R_H evaluation.

IV. CONCLUSION

The analysis of typical marks and impressions on the cartridge case image is very important evidence in courts. Due to the limitation of image acquisition device and the unsmooth specimen surface, we have focused on cartridge case image mosaic which is used to stitch several cartridge case images into one, so that experts' analysis and computer processing are really facilitated. Because of the similar texture of cartridge cases, the SIFT algorithm has incorrect matches which greatly affect the registration accuracy, and the traditional method of removing incorrect matches bears unsatisfactory results. Therefore, according to the character of cartridge case images, the voting mechanism that combines GTM, angle and scale constraint algorithm is applied to remove incorrect matches effectively, and registration accuracy is enhanced. Ultimately, the stitched image contains more information than that of each of the original images. Experimental results show that proposed method outperforms typical approach in terms of visual appearance and objective evaluations. In addition, depending on specific issues, future work will expand the use of this voting mechanism by conducting other methods.

ACKNOWLEDGMENT

This work is supported by the Science Foundation for Young Teachers of Northeast Normal University, (No. 20090302), the Key Project of MOE (No. 109052), the

Training Fund of NENU'S Scientific Innovation Project (No. NENU-STC07018), the Fund of Jilin Provincial Science & Technology Department (No. 20070322), the NSFC (No. 10871037).

REFERENCES

- [1] F. Puente León, "Automated comparison of firearm bullets," *Forensic Science International*, vol.156, 2006, pp. 40-50.
- [2] Patrick De Smet, Rob Hermsen, Bert van Leuven, Jan De Kinder, Kai Hoffmann, "Experimental evaluation of the impact of seating depth variations on observed marks on primers," *Forensic Science International*, vol.179, 2008, pp. 163-171.
- [3] C.Y. Wen, J.K. Chen, "Multi-resolution image fusion technique and its application to forensic science," *Forensic Science International*, vol.140, 2004, pp. 217-232.
- [4] Alec Mills, Gregory Dudek, "Image stitching with dynamic elements," *Image and Vision Computing* doi:10.1016/j.imavis.2009.03.004.
- [5] Bin Ma, Timo Zimmermann, Manfred Rohde, Simon Winkelbach, Feng He, Werner Lindenmaier, Kurt E.J. Dittmar, "Use of autostitch for automatic stitching of microscope images," *Micron* 38 2007, pp. 492-499.
- [6] Krystian Mikolajczyk and Cordelia Schmid, "A performance evaluation of local descriptors," *IEEE Transactions on Pattern Analysis and Machine Intelligence*, vol. 27, no. 10, October 2005, pp. 1615-1630.
- [7] Lowe, D G, "Distinctive image features from scale-invariant keypoints," *International Journal of Computer Vision* 60(2), 2004, pp. 91-110.
- [8] Le Yu, Dengrong Zhang, Eun-Jung Holden, "A fast and fully automatic registration approach based on point features for multi-source remote-sensing images," *Computers & Geosciences*, vol.34, 2008, pp. 838-848.
- [9] Wendy Aguilar, Yann Frauel, Francisco Escolano, M. Elena Martinez-Perez, Arturo Espinosa-Romero, Miguel Angel Lozano, "A robust Graph Transformation Matching for non-rigid registration," *Image and Vision Computing* vol. 27, 2009, pp. 897-910.
- [10] Richare O.Duda, Peter E. Hart, David G.Stork, *Pattern Classification (Second Edition)*, 2007, Publishing China Machine Press, pp.423-424.
- [11] Shuai Wang, Jiafeng Liu, Jianhua Huang, Xianglong Tang, Da Sun, "A Method of Image Registration based on Adaptive Clustering," *Microcomputer Information in Chinese* 1008-0570, 2008, 04-3-0288-02.
- [12] D.E. Goldberg, "Genetic Algorithms in Search, Optimization and Machine Learning," Addison-Wesley, Reading, MA, 1992.
- [13] Rafael C. Gonzalez, Richard E. Woods, *Digital Image Processing (Second Edition)*, Publishing House of Electronics Industry, 2002, pp. 74-80.
- [14] C. Studholme, D.L.G. Hill, D.J. Hawkes, "An overlap invariant entropy measure of 3D medical image alignment," *Pattern Recognition* vol, vol.32, 1999, pp.71-86.
- [15] Q.S. Chen, M. Defrise, and F. Deconinck, "Symmetric phase-only matched filtering of Fourier-Mellin transforms for image registration and recognition," *IEEE Trans. Pattern Analysis and Machine Intelligence*, vol. 16, no. 12, 1994, pp. 1156 - 1168.
- [16] B. S. Reddy and B. N. Chatterji, "An FFT-Based technique for translation, rotation, and scale-invariant image registration," *IEEE Trans. Image Processing*, vol. 5, no. 8, 1996, pp. 1266-1271.
- [17] Wei Huang, Zhongliang Jing, "Evaluation of focus measures in multi-focus image fusion," *Pattern Recognition Letters* 28, 2007, pp.493-500.

- [18] Phen-Lan Lin, Po-Ying Huang, "Fusion methods based on dynamic-segmented morphological wavelet or cut and paste for multifocus images," *Signal Processing* 88, 2008, pp. 1511-1527.



information fusion.

Man Luo was born in Tianjin, China. She received her B.S and M.S degrees from Computer School of Northeast Normal University, China, in 2005 and 2010, respectively. Now she is a teacher in College of Air Traffic Management, Civil Aviation University of China. Her main research interests are digital image processing, pattern recognition and



Miao Qi was born in Liaoning, China. She received her B.S and M.S degrees from Computer School of Northeast Normal University, China, in 2004 and 2007, respectively. She received the Ph.D. degree from Faculty of chemistry, Northeast Normal University, in 2010. Now, she is a teacher in School of Computer Science and Information Technology, Northeast Normal University. Her main research interests are digital image processing, pattern recognition and chemistry computation.